Microfluidic preparative free-flow isoelectric focusing in a triangular channel: System development and characterization

Published in final edited form as:
Electrophoresis. 2010 May ; 31(10): 1606–1614. doi:10.1002/elps.200900577.

Microfluidic Preparative Free-Flow Isoelectric Focusing in a Triangular Channel: System Development and Characterization

Jian Wen, **Jacob Albrecht**[1], and **Klavs F. Jensen**[*]
Department of Chemical Engineering, Massachusetts Institute of Technology, 77 Massachusetts Avenue, Cambridge, MA 02139

Abstract

A preparative scale free-flow isoelectric focusing (FF-IEF) device is developed and characterized with the aim of addressing needs of molecular biologists working with protein samples on the milligrams and milliliters scale. A triangular-shape separation channel facilitates the establishment of the pH gradient with a corresponding increase in separation efficiency and decrease in focusing time compared to that in a regular rectangular channel. Functionalized, ion-permeable poly (acrylamide) gel membranes are sandwiched between poly (dimethyl silxoane) (PDMS) and glass layers to both isolate the electrode buffers from the central separation channel and also to selectively adjust the voltage efficiency across separation channel to achieve high electric field separation. The 50 × 70 mm device is fabricated by soft lithography and has 24 outlets evenly spaced across a pH gradient between pH 4 and 10. This preparative FF-IEF system is investigated and optimized for both aqueous and denaturing conditions with respect to the electric field and potential efficiency and with consideration of Joule-heating removal. Energy distribution across the functionalized polyacrylamide gel is investigated and controlled to adjust the potential efficiency between 15 - 80% across the triangular separation channel. The device is able to achieve constant electric fields high as 370 ± 20 V/cm through the entire triangular channel given the separation voltage of 1800 V, enabling separation of five fluorescent pI markers as a demonstration example.

Keywords

Microfluidic; Preparative; Free flow; Electrophoresis Isoelectric focusing (IEF)

1 Introduction

In order to address the complex protein composition of whole cell lysate, proteomic approaches depend on the ability to separate proteins across multiple dimensions. Isoelectric focusing (IEF) segregates amphoteric molecules by their isoelectric point (pI) independent of hydrophobicity or size. In free-flow IEF (FF-IEF), a sample solution is pumped through a chamber, and an electric field is applied perpendicular to the fluid flow. FF-IEF is best suited as a preparative technique, as it can crudely fractionate large samples while maintaining protein chemical and biological activity. In recent years, simple, disposable miniaturized FF-IEF devices have emerged as a promising tool for crude sample preparation prior to subsequent separations.

[*] Corresponding author: kfjensen@mit.edu. Phone: 617-253-4589. Fax: 617-258-8992.
[1] Current address: Chemical Technologies, Process Research and Development, Pharmaceutical Research Institute, One Squibb Drive, New Brunswick, NJ 08903

Yager and coworkers [1,2] developed FF-IEF microdevices to concentrate bacteria cells or proteins in a straight microfluidic channel. Since the electrodes were in direct contact with the separation liquid, the devices were operated at a very low voltage of 2.6 V (2.04 V/cm) to avoid the bubbles generated by electrolysis. Yang et al [3] coated the PDMS channel with glass through TEOS-sol gel process and was able to concentrate the model protein of RFP and EGFP around 214 μm and 357 μm from the anode, respectively. Glass coating was found to help stabilize the device running from electrolysis but require twice time to focus the sample. An electric potential of 1.5 V/cm was reported upon focusing optimization. Xu et al.[4] reported FF-IEF devices using an array of narrow side channels to connect the straight separation channel with the electrode buffer reservoirs, which was similar to an earlier report of free-flow electrophoresis (FFE) device on silicon [5]. Only ~4% of the applied voltage (1,750 V) was applied to the separation chamber with an electric field of 135 V/cm due to the high resistance from the side channels. High voltage potential of up to 4,000 V was reported before bubbling became significant problems. To improve the voltage efficiency across the side connecting channels, Fonslow et al.[6] further increased the channel dimensions and raised the voltage efficiency to 50% in a glass microfluidic device. A high electric field of up to 283 V/cm across the separation channel was reported, which enabled the good separation of fluorescein and rhodamine. By eliminating the side connecting channels, a higher voltage efficiency of up to 91% was achievable on a glass chip [7, 8], generating the high electric field up to 586 V/cm. All channels were connected directly with each other but the electrode buffer channels were etched 4-times deeper than separation channel. With a 16 times higher volume flow-rate of electrode buffer than that in separation channel, the linear velocity of all flows were kept the same and electrolysis bubbles were efficiently removed.

Different physical matrix structures have been used to isolate the electrode buffer bubbles from separation channel. Janasek et al.[9] adapted thin dielectric barriers within a glass microfluidic chip to transfer the charges and generate the electric field. Potential efficiency of 50% was reported across the separation channel with a corresponding electric field of up to 180 V/cm. Kohlheyer et al.[10, 11] integrated ion-permeable UV-polymerized polyacrylamide membranes into the glass chips. Voltage efficiency was estimated between 40% and 60% across the 1.5 mm wide channel with a reported electric field of 250 V/cm. Separation of four fluorescent IEF markers was demonstrated at a flow rate of 1.2 μL/min. We have also reported earlier the use of functionalized gel electrodes and cascaded focusing stages to apply over 200 V/cm to focus cell lysate at a rate of 5 μL/min[12,13]. Operating without sheath flow near the electrodes, the devices had a voltage efficiency estimated to be approximately 30%. For a more thorough understanding of the micro FFE modes and the development of IEF at the microscale, we refer recent review articles [14, 15]

Disposable, inexpensive IEF devices have the potential to become a useful tool for research involving difficult proteins and protein complexes, reducing laborious sample preparation and increasing assay sensitivity. For preparative separations on the milliliter scale, current FF-IEF tools require carefully cleaned and manually assembled apparatus to perform separations. These tools use multiple inlets to create a pH gradient across the width of the device [16, 17]. These inlets in turn require multiple premixed proprietary pH buffers, a dedicated pumping system, and increased system cost and complexity. A sample introduced to this multiple buffer system is instantly diluted, reducing detection sensitivity even after focusing. Previous reports [1-15, 18] have described devices with volumes in the range of less than 2 μL. However, the flow rates are too low to process typical sample volumes (milliliters) experienced in biological research. In addition, in order to perform practical bioseparations, FF-IEF micro devices must physically fractionate as many outlet streams as possible.

We have designed and optimized an efficient microfluidic device with a novel triangular separation channel design to perform fast free-flow IEF separation of preparative-scale with a sample separation rate of at least 10 μl/mL or higher. Ion-permeable polyacrylamide gel membranes are sandwiched between the poly(dimethyl siloxane) (PDMS) and glass layers to both isolate the electrode buffers from the central separation channel and also to selectively adjust the voltage efficiency across separation channel for high electric field separation. Optimization of the poly (acrylamide) gel size is performed and found to be critical for the best performance of the microdevice. Separation of fluorescent IEF pI markers served as a model system. With this optimized system, it becomes possible to explore the separation of complex protein mixtures as demonstrated elsewhere [19].

2 Materials and methods

2.1 Reagents and chemicals

All water used in this work has been pre-purified by a Milli-Q Academic (Millipore, Billerica, MA) equipped with an extra 0.22 μm membrane filter. Tris(hydroxymethyl)aminomethane (Tris, 99.9+%), 3-(trimethoxysilyl)propyl methacrylate (98%+), 2,2- dimethoxy-2-phenylacetophenone (DMPA), poly (vinyl alcohol) (PVA, M_w 89,000 ~ 98,000, 99+%), urea (99.5+%), thiourea (99+%), CHAPS (98+%), Methyl Red, Bromothymol Blue, Nonidet P 40 substitute (NP-40), 10× PBS buffer, ethanol (95%), acetone, Phosphoric acid (85%), acetic acid (≥99.7%), Triton X-100, Ampholytes 3-10, mineral oil, fluorescently labeled pI markers of pI 4.5 (λ_{ex} 336 nm, λ_{em} 424 nm), pI 5.5 (λ_{ex} 325 nm, λ_{em} 412 nm), pI 6.8 (λ_{ex} 338 nm, λ_{em} 418 nm), pI 7.6 (λ_{ex} 385 nm, λ_{em} 495 nm), and pI 9.5 (λ_{ex} 325 nm, λ_{em} 415 nm) were obtained from Sigma Aldrich (St. Louis, MO). Poly(dimethylsiloxane) (PDMS, Sylgard 184, Dow Chemicals, Midland, MI) kit was obtained from Ellsorth Adhesives (Germantown, WI). Acrylamide monomer solutions (PlusOne ReadySol IEF), Immobilines of pK 3.6 and pK 9.3 were obtained from GE Healthcare, Piscataway, NJ. 10× Cathode electrode buffer was obtained from Bio-rad Laboratory (Hercules, CA).

2.2 Device fabrication

The device (Figure 1) was fabricated using standard soft lithography techniques [20]. A mold was created from the photopatternable polymer SU-8 2050 (MicroChem, Newton, MA) spin-cast on a featureless 4” silicon wafer with a uniform thickness of 160 μm. The SU-8 was exposed to UV through a transparency mask to transfer the features. Fabrication of PDMS device was performed in two steps. A small amount of PDMS (~10 g) was first poured over the mold (~2-3 mm in thickness) and cured at 80°C until solid (~20 min). A supporting glass slide was positioned above the first layer and held in place with a magnet. More PDMS (~20 g) was poured and allowed to completely cure (Figure 1A). The shape of the supporting glass slide varied as long as it has covered the majority of the channel to prevent channel sagging. After the device was cut and peeled from the master, access holes (one inlet, 24 outlets) were punched using a blunt-end 20 gauge Luer stub adapter (Becton-Dickinson, Sparks, MD). To adjust the ratio of the applied potential across the separation channel, the PDMS layer was shaped by removing excess regions on sides. The PDMS surface was cleaned using cellophane tape prior to sealing.

The PDMS/glass device was sealed by surface oxidation in oxygen plasma (Harrick, Ithaca, NY). A double-wide microscope slide (75 × 50 mm, Erie Scientific, VWR) was first exposed to plasma for 65 sec, and then for another 45 sec together with the PDMS layer. The glass was brought into contact with the PDMS surface to form a permanent bond. The PDMS/glass device was then filled with 1% 3-(trimethoxysilyl)propyl methacrylate in ethanol with pH adjusted to ~5 using 6 M acetic acid (~ 1 % v/v) for 1 hr. All the devices

were dried, degassed in vacuum overnight at 80°C, and then transferred to an acrylic nitrogen glove box (Air Control, Inc., Henderson, NC) for poly (acrylamide) gel casting. Stock anode and cathode monomer acrylamide gel solution were prepared by mixing 9 mL acrylamide monomer solution containing 40% w/v acrylamide monomer and 3% w/w N,N′-methylenebisacrylamide, 13.5 mL Milli-Q water, and 1.5 mL Immobiline pK 3.6 (stock in water) or Immobiline pK 9.3 (stock in 2-proponal), respectively. Stock gel solutions were stored at 4°C for reuse. Photo initiator was mixed with the acrylamide gel solution right before the polymerization. Polymerization working solution was prepared by adding 6 μL of 10% DMPA (photo initiator) to every 1 mL of the stock monomer solution right before the polymerization step. An extra of 24 μL of 1% v/v Triton X-100 was added to every 1 mL of anode polymerization solution. The monomer solutions were introduced into the edges of the device and pulled through the PDMS/glass device by capillary action before it was held by surface tension at the hydrophobic channel-gel region barriers (a series of posts with 40 μm spacing). It is very critical to control the overall hydrophobicity of the polymerization solution (volume of Triton added) so that it will not cross the barriers to the central focusing chamber during the polymerization step. The acrylamide was polymerized by exposure to long-wave UV (365 nm, Spectroline ENF-280C, Spectronics Corporation, Westbury, NY) for 3 min (Figure 1B). Cathode and anode gels were processed separately in no preferred order. The devices were stored under 2% (w/v) PVA solution. To investigate the effect of electrode functionalized gel, potential drop across the triangular separation channel was measured in selected experiments. The regular shape of the supporting glass slide during PDMS fabrication was temporarily replaced with a triangular glass slide that was slightly smaller than the separation channel to allow for external access to the channel solution through the PDMS layer. Each side of the channel along the channel edge was manually perforated with 16 holes through the PDMS layer using a 20 gauge Luer stub needle (Becton-Dickinson, Sparks, MD), with the first point located ~0.9 cm from the inlet, the last point placed ~0.2 mm from the outlet, and all points spaced 0.32 cm (0.125 inch) apart. Care was taken to reproducibly punch the holes from device to device to lower the detection variation. Two blunt-end 20 gauge Luer adapters were then inserted through the holes to reach the channel solution during selected experiments, and potential drops between either the two adapters or between the electrode and buffer were measured using a voltmeter. Safeguards were used to ensure safe voltage measurements.

2.3 Device operation

The setup of the FF-IEF system is shown in Figure 2. Two strips of 2”-wide Scotch tape were attached to the device edges to prevent a potential short circuit. Two custom containers made from PDMS with immobilized platinum electrodes were then glued to the sides of the device to hold either 1× cathode (20 mM Arginine, 20 mM Lysine) or anode electrode buffer (0.1 M H_3PO_4). The connections between the device and containers were sealed with 5-minute epoxy glue (Devcon, Danvers, MA) to isolate the electrode buffers. The device was placed atop a thermoelectric cold plate with a temperature controller (CP-036 and TC-24-10, TE Technology, Inc., Traverse City, MI) to efficiently remove the generated Joule heat and to maintain the devices at 2°C. Mineral oil was applied between the cooling plate and device for improved heat transfer and for the prevention of a possible short circuit. Samples were delivered into the device via a syringe pump (Cole-Parmer, Vernon Hills, IL), and the device was powered by a high-voltage power supply (EPS 3501, GE Healthcare, Sweden). Twenty-four 200-μL gel loading capillary pipette tips (VWR, West Chester, PA) were inserted into the PDMS to collect the outlet fractions. The fine plastic capillary of the pipette tip fit snugly into the 20-gauge hole, and was held in place without leaks for the duration of the experiment.

2.4 Sample preparation and image analysis

Different buffers were used in this work. Aqueous sample buffer was prepared as 50 mM Tris, 2% PVA, and 2% Fluika ampholytes 3-10, pH 7.5. Methyl Red and Bromothymol Blue (0.1% each in final concentration) were used in some of the experiments to indicate the pH gradient. Urea-based denaturing sample buffer was prepared as 8 M urea, 2 M thiourea, 4% CHAPS, 4% PVA, and 2% ampholytes. For investigation of separation channel shape, a buffer of 0.5× PBS, 60 ppm Bromothymol Blue, 250 ppm Methyl Red, 0.8% CHAPS, 0.5% NP-40, and 2% ampholytes was used. To visualize the device separation, 5 fluorescently labeled pI markers were mixed in the urea sample buffer. The final concentration of each marker and its fluorescence properties were: pI 4.5 (50 μg/mL, λ_{ex} 336 nm, λ_{em} 424 nm), pI 5.5 (150 μg/mL, λ_{ex} 325 nm, λ_{em} 412 nm), pI 6.8 (50 μg/mL, λ_{ex} 338 nm, λ_{em} 418 nm), pI 8.7(50 μg/mL, λ_{ex} 390 nm, λ_{em} 500 nm), and pI 9.5 (50 μg/mL, λ_{ex} 325 nm, λ_{em} 415 nm). The fluorescent sample mixture was loaded into the device with a constant flow rate of 10 μL/min, and a constant voltage of 1,800 V was applied. Fluorescence images were taken by a Canon PowerShot S51S digital camera under long-wave UV light of 365 nm.

3 Results and discussion

3.1 Optimization of separation channel shape

For the case of IEF in a diverging channel, the relationship between focusing time and channel distance is no longer linear since the fluid slowing as it enters a progressively larger channel. Assuming uniform flow across the width of the channel at all times, the relationship between channel distance and focusing time can be derived.

For a symmetric, linearly diverging channel with angle α on each side and with initial width w_0 and length L, the channel width as a function of length, w, is defined by.

$$w=2L\tan(\alpha)+w_0 \tag{1}$$

Assuming an inlet velocity of U_0, and uniform flow across the width of the channel, the rate that liquid will flow down the length of the channel at a given time is assumed to diminish proportionately with a change in w, as given by:.

$$\frac{dL}{dt}=U(t)=\frac{U_0w_0}{w}=\frac{U_0w_0}{2L\tan(\alpha)+w_0} \tag{2}$$

The assumption of uniform flow is valid when there is sufficient external pressure on the outlets of the device. The rate that the channel diverges is then

$$\frac{dw}{dt}=2\tan(\alpha)\frac{dL}{dt}=2\tan(\alpha)U(t)=\frac{2\tan(\alpha)U_0w_0}{2L\tan(\alpha)+w_0}=\frac{2\tan(\alpha)U_0w_0}{w} \tag{3}$$

Integrating and solving for w yields a relationship between channel width and residence time

$$w(t)=\sqrt{\left(4\tan(\alpha)\,U_0w_0t+w_0^2\right)} \tag{4}$$

Thus for a channel diverging linearly in space, the fluid inside will experience a change in channel width with respect to the square root of time. A free-flow IEF numerical simulation was used to examine the effects of diverging channel geometry on focusing dynamics [21].

The preparative FF-IEF device was designed with the goal of fractionating a sample into 24 outlets with a throughput of up to 1 mL/hr. Because of the large number of outlets and also the high throughout rate demanded, cascaded FF-IEF stages in our previous report [13] would quickly become too cumbersome to fabricate (up to 9 outlets) and limited in flow rate (less than 1 μL/min). Therefore, a new approach was taken to design these preparative-scale devices. The device is a single stage with a diverging channel, offering the benefits of the cascaded approach without a prohibitively large and intricate footprint. As the size of the device increased, the soft, rubbery PDMS was found to sag during device sealing. Previous reports [5, 6, 9] have incorporated post structures in the separation channel to prevent channel sagging. Here, we introduce a glass platform, a double-wide microscope side cut to match the channel dimensions was cured inside of the device PDMS layer, lending rigidity to the devices while retaining the advantages of soft lithography fabrication.

Comparison the new divergent channel design with a conventional rectangular layout serves to illustrate the advantages of a diverging sample channel (Figure 3). The rectangular device (Figure 3A) has up to three optional inlets for sheath flow, similar to other FF-IEF designs [2-18, 22]. The central inlet of the rectangular device design uses a branched structure defined by PDMS posts (white diamonds) to balance the pressure drop and flow rate across the width of the channel. The second design consists of a single inlet with a linearly diverging channel (Figure 3C).

Comparison of the formation of a pH gradient in each of the two designs (Figure 3), as reflected by a mixture of Methyl Red and Bromothymol Blue in the sample buffer reveals that development of the pH gradient is much slower in the rectangular channel than in the diverging channel design. Since pH gradient formation begins at the gel-channel interface, any rectangular device or with a single inlet will necessarily have a pH-gradient development region commensurate to the channel width. In the case of the design in Figure 3A, the time for the sample to respond and establish a pH gradient across the width of the channel is only slightly less than residence time of the device. Moreover, the applied voltage (electric field ≈ 90 V/cm) is sufficient high to cause electrokinetic disturbances in the flow, appearing as color “wrinkles” near the cathode. In contrast, the divergent channel quickly establishes a pH gradient at the narrow inlet, which is continually refined as the channel diverges. Electrokinetic disturbances in the divergent channel were markedly reduced, and the device was less sensitive to higher applied voltages. The rapid initial focusing also allowed for much higher flow rates; residence times as low as 1 min were observed to produce similar color gradients. Both devices showed some cathodic shift due to electroosmotic flow (EOF), since no dynamic coating reagents (e.g., PVA) were included in the running buffer. Owing to the much higher efficiency of the diverging triangular shape channel design in pH gradient generation and focusing time, it was adapted for the preparative scale separation.

3.3 Balance of pressure drop

The fluid velocity through the diverging channel device is discussed by Denn [23]. In the channel height dimension the flow field shows the usual parabolic form, but the average fluid velocity decreases with the inverse of the distance from the inlet rather than being constant as in a rectangular channel. For small divergence angles (α) the flow velocity fluid flow takes the form:

$$v_r(r,z)=\frac{3q}{2\alpha r}\left(1-\left(\frac{z}{H}\right)^2\right) \quad (5)$$

as a function of channel height *z*, in a chamber with a total height of 2*H*. Here, the distance from the inlet is given by *r*, and *q* represents the cross-sectional velocity (m^2/s), constant throughout the chamber. Figure 4A shows a finite element simulation of the pressure distribution in a half section of the channel.

Because the outlets are not equidistant from the inlet, they will experience non-uniform fluidic resistances, and the challenge of achieving uniform outlet flow rates increases with the number of outlets. The hydrostatic pressure in the outlet pipettes was used to even out flow variations among the outlets. During device operation, faster filling outlets created a larger hydrostatic pressure than slower outlets with a resulting reduction in flow into the fast lanes. This hydrostatic pressure negative feedback to the central outlets promoted an equal volume collection of the outlet fractions (Figure 4B). Even flow was observed until flow rates greater than 2 mL/hr were applied, in which case a parabolic flow profile was observed with more fluid in the central portion.

3.4 Optimization of device design for high electric fields under aqueous condition

After demonstrating the advantages of a triangular separation channel and even flow for sample collection, we further investigated the device electric field and its effect on separation efficiency under an aqueous buffer condition. The inlet region with the narrowest part of the separation channel is the region with the highest electrical current, since many more molecules coming just from the inlet are still charged and travel towards their isoelectric points. As the analytes travel towards the outlets, electrical current is low and mostly caused by molecules leaving the isoelectric point region due to diffusion and the slightly changing pH gradient as the channel being wider and pH gradient being reestablished, which is then counteracted as the molecules gets charged again.

To determine the potential across the triangular channel at different sites, a series of holes (16) were temporarily punched along the channel on both sides, and two blunt-end syringe Luer adapter were inserted to reach the channel solution (160 μm in channel depth) (Figure 5A). Potential drops across both the anode (V1) and cathode (V3) functionalized gels and across the separation channel (V2) were quickly read 3 times directly from a voltmeter and averaged. Slow solution purge was observed but did not affect the reading. Potential efficiency (Figure 5C) was calculated as ratio of V2 over the total applied voltage (V1+V2+V3), ranging from 0 - 100%. Electric fields (Figure 5D) were calculated by dividing the measured horizontal V2 over the relative channel width. The full scale of the device without any removal of PDMS prior to device binding was first investigated. The x-axis value shows the distance of the reading holes to the inlet. As shown in Figure 5C (square line), potential efficiency up to 70% was applied directly to the separation channel, generating a high electric field in regions close to the outlet of up to 260 ± 15 V/cm when a 1500 V potential was applied. However, a relatively large ratio of the applied potential was found to be lost on the functional gels on both sides of the inlet region, resulting in a relatively low potential across the channel and low electric field (as low as only ~2 V/cm). This increasing electric field mode favors stronger focusing force as a sample flows toward the outlets, but at the expense of separation efficiency due to the long time required for sample focusing when it was initially loaded. To improve the potential efficiency, we modified the shape of the functionalized electrode gel to achieve a specific potential drop variation across the central separation channel. Since the potential was expected to increase proportionally with the gel length, we started with the strip scale design (Figure 5B-b) where

a constant gel width of 5 mm was included, except for the top corners (~ 2 mm) which were constrained by the size of the glass layer upon device binding. Cross-channel potential efficiency in Figure 5C (triangle line) was observed to be much higher compared to that in the full-scale design. A maximal potential of between 500 to 600 V (~ 4 mA) was applied before boiling was observed near the inlet region since this region has the highest electrical current after sampling load. The electric field was found to quickly drop from 300 ± 10 V/cm (n = 3) close the inlet to only 100 ± 10 V/cm (n = 3) near the outlets. This decreasing field strength improved focusing time when the sample was initially loaded, but with the decrease in field with length a focused sample might defocus as it travels to the outlets. Keeping the gel width at the top starting at 5 mm constantly, further investigations of the gel width on bottom were carried for achieving maximal constant electric field, finally arriving at an optimized width of 12 mm (Figure 5B-c). As shown in Figure 5C (diamond line), with the selected potential efficiency of 75% (top) to 17% (bottom), a constant electric field of 300 ± 25 V/cm (1500 V applied potential, ~3 mA current) was measured within the entire separation channel.

3.5 Urea denaturing condition

Having shown the device to be capable of constant electric fields in aqueous buffers, we next tested the device in denaturing buffer conditions. One of the advantages of using the denaturing buffer over the aqueous buffer is the low salt and water concentration that affords a much lower current compared to the aqueous medium when the same potential is applied; thus, a higher voltage can be applied to the device and generate even higher electric fields. As shown in Figure 6, cross-channel potential efficiency was found to be very similar to what we have shown in Figure 5, with 80 ± 5% on top and 15 ± 3% (n = 5) selectively on the bottom. Uniform electric fields have also been achieved as high as 370 ± 20 V/cm when 1800 V was applied (2.0 mA cutoff current for system stability). Spatially uniform fields were also observed with lower applied voltage. Potentials as high as 2200 V could be applied to the device, but only for ~10 min before the solution was observed to boil in the bottom region. As a result, the device was operated under a cutoff voltage of 1800 V with a typical electric field of 370 ± 20 V/cm and a cutoff current of 1.5 -1.9 mA, whichever came first.

3.6 Separation of fluorescent pI markers

After the FF-IEF system was optimized to achieve high electric fields through the divergent channel, a mix of 5 fluorescent pI markers (pI 9.5, 8.7, 6.8, 5.5, 4.5) were separated and visualized with exposure to long-wavelength UV light (365 nm). As shown in Figure 7, a sharp separation was observed with a flow rate of 10 μL/min. The intensity of the markers varied because of their different excitation wavelengths and concentration. Highly focused samples are observed in fraction 4, 11 and 15. A pH gradient range of 4 to 10 was achieved through the 24 outlet fractions, thus brings the device resolution to as low as 0.25 pH per fraction. It is also worthwhile to note the efficient focus shown by the fluorescent markers in the sample inlet region. With 24 different fraction outlets, distributions between neighboring outlets of markers that separated at the boundary between two outlet regions become sensitive to small variations in flow rates. As an example of this phenomenon, the pI 6.8 marker of varied between fractions 10 and 11 during flow. Variations of the flow path were sometimes also observed owing to the dynamic establishment of the pH gradient during the continuous loading mode, change of the flow rate, effect from EOF, or uneven surface of the master wafer for PDMS production. Designed as a pre-fractionator for macro scale protein separation, the markers are demonstrated well separated into different outlets confirming the potential of the system for separating protein mixture and whole cell lysate, as demonstrated elsewhere [19].

4 Conclusions

In this work, a novel preparative scale FF-IEF device with one inlet and 24 outlets has been developed and characterized. Relative to conventional rectangular designs, the divergent IEF channel has the advantage of faster the formation of pH gradients and with the proper design of the electrode regions, uniform potential drops along the length of the channel. By shaping of the PDMS prior to the device binding, the poly (acrylamide) gel region could be adjusted to achieve a ratio of the applied potential across the separation channel between 15% and 80%. High and nearly uniform electric fields of up to 370 ± 20 V/cm under denaturing buffer conditions were thus achieved in the device and contributed to sharp separation of fluorescent marker mixtures. Denaturing conditions can in principle be applied to biological samples and other complex protein mixtures. However, separation conditions, such as flow rate, surface coating, and separation resolution still need further optimization for specific applications [19].

Acknowledgments

Funding for this work was provided by U.S. Army Research Office under contract W911NF-07-D-0004 and NIH grant GM68762.

References

1. Cabrera CR, Yager P. Electrophoresis. 2001; 22:355–362. [PubMed: 11288905]
2. Macounov K, Cabrera CR, Yager P. Anal Chem. 2001; 73:1627–1633. [PubMed: 11321320]
3. Yang KS, Clementza P, Parka TJ, Leed SJ, Park JP, Kim DK, Lee SY. Current Applied Physics. 2009; 9:e66–e70.
4. Xu Y, Zhang C, Janasek D, Manz A. Lab Chip. 2003; 3:224–227. [PubMed: 15007450]
5. Raymond DE, Manz A, Widmer HM. Anal Chem. 1994; 66:2858–2865.
6. Fonslow BR, Bowser MT. Anal Chem. 2005; 77:5706–5710. [PubMed: 16131085]
7. Fonslow BR, Barocas VH, Bowser MT. Anal Chem. 2006; 78:5369–5374. [PubMed: 16878871]
8. Fonslow BR, Bowser MT. Anal Chem. 2006; 78:8236–8244. [PubMed: 17165812]
9. Janasek D, Schilling M, Manz A, Franzke J. Lab Chip. 2006; 6:710–713. [PubMed: 16738720]
10. Kohlheyer D, Besselink GAJ, Schlautmann S, Schasfoort RBM. Lab Chip. 2006; 6:374–380. [PubMed: 16511620]
11. Kohlheyer D, Eijkel JCT, Schlautmann S, van den Berg A, Schasfoort RBM. Anal Chem. 2007; 79:8190–8198. [PubMed: 17902700]
12. Albrecht JW, Jensen KF. Electrophoresis. 2006; 27:4960–4969. [PubMed: 17117380]
13. Albrecht J, El-Ali JW, Jensen KF. Anal Chem. 2007; 79:9364–9371. [PubMed: 17994708]
14. Kohlheyer D, Eijkel JCT, van den Berg A, Schasfoort RBM. Electrophoresis. 2008; 29:977–993. [PubMed: 18232029]
15. Sommer GJ, Hatch AV. Electrophoresis. 2009; 30:742–757. [PubMed: 19260009]
16. Burggraf D, Weber G, Lottspeich F. Electrophoresis. 1995; 16:1010–1015. [PubMed: 7498121]
17. Weber G, Bocek P. Electrophoresis. 1996; 17:1906–1910. [PubMed: 9034773]
18. Guillo C, Karlinsey JM, Landers JP. Lab Chip. 2007; 7:112–118. [PubMed: 17180213]
19. Wen, J.; Wilker, EW.; Yaffe, MB.; Jensen, KF. Anal Chem. ASAP;
20. Duffy DC, McDonald JC, Schueller OJA, Whitesides GM. Anal Chem. 1998; 70:4974–4984.
21. Albrecht, JW. PhD Thesis. Massachusetts Institute of Technology; 2008.
22. Wu D, Luo Y, Zhou X, Dai Z, Lin B. Electrophoresis. 2005; 26:211–218. [PubMed: 15624173]
23. Denn, MM. Process Fluid Mechanics. Prentice-Hall; Englewood Cliffs, NJ: 1980.

Abbreviations

IEF	Isoelectric focusing
FFE	free-flow electrophoresis
FF-IEF	free-flow isoelectric focusing
PDMS	poly (dimethyl silxoane)
pI	isoelectric point
TEOS	Tetraethyl orthosilicate
DMPA	2,2- dimethoxy-2-phenylacetophenone
PVA	poly (vinyl alcohol)
PBS	phosphate buffered saline
EOF	electroosmotic flow

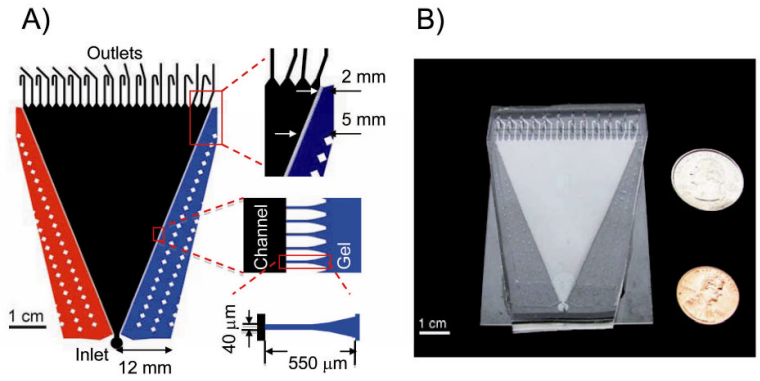

Figure 1.

A) Mask design and B) photograph of the FF-IEF device. The functionalized pH gradient cathode (pK = 9.3, red) and anode (pK = 3.6, blue) polyacrylamide gels were polymerized into the gel regions, separated from the separation channel by a series of 40 μm wide channels. Both polyacrylamide gel sections were cut to 5 mm from the first post on the top and 12 mm from the inlet to the side on the bottom. The separation channel was perforated with 32 holes for potential and local temperature measurement in selected experiments. The device measures 50 mm by 75 mm, with the central triangular separation channel of 46 mm wide at the top and 56 mm long. All channels are 160 μm deep.

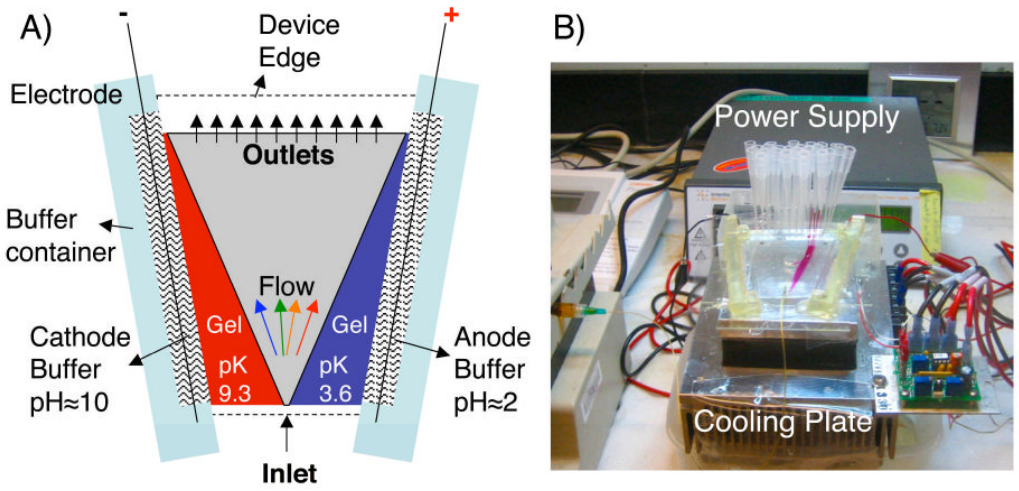

Figure 2.
A) Schematic drawing of the microfluidic FF-IEF system and B) image of the operation setup.

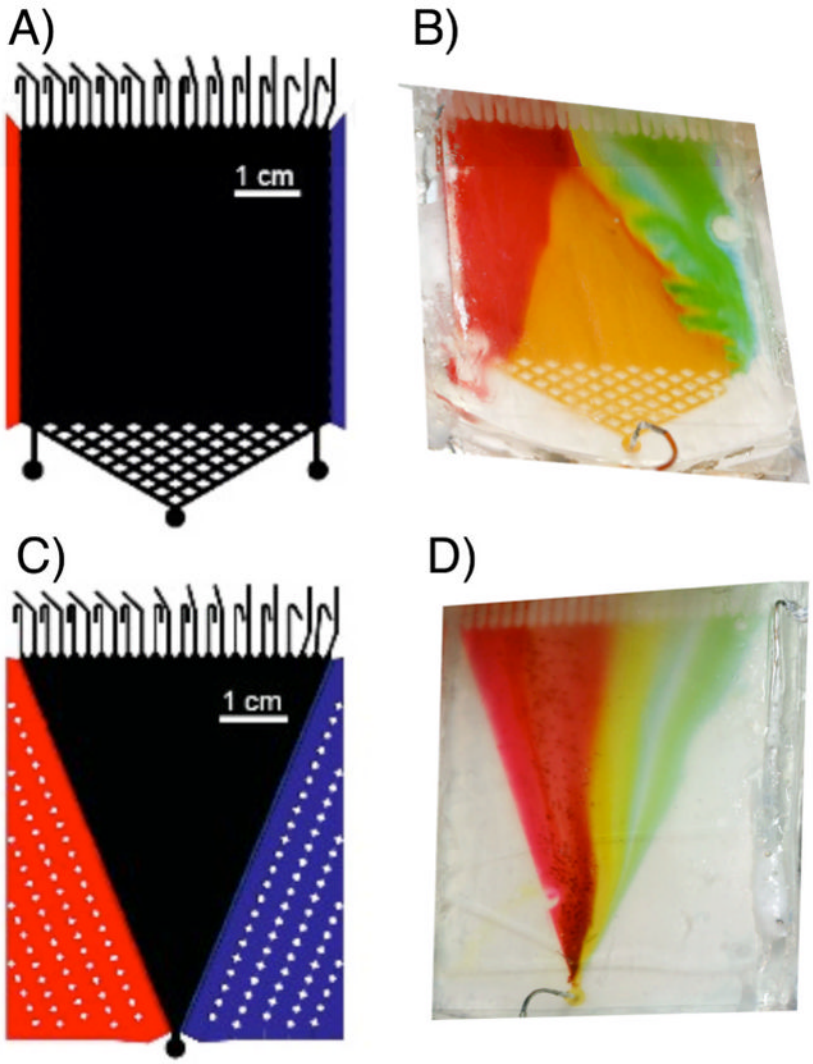

Figure 3.

Comparison of rectangular and divergent designs for separating a mixture of Methyl Red and Bromothymol Blue. The color gradient indicates the presence of an established pH gradient. Both devices were operated at 480 V and a residence time of 6.5 min. Sample buffer: 0.5× PBS, 60 ppm Bromothymol Blue, 250 ppm Methyl Red, 0.8% CHAPS, 0.5% NP-40, and 2% ampholytes. Current: ~8 mA. Channel dimensions: rectangular 47 mm (w), 45 mm (L), 165 μm (D), and 348 μL (vol); triangular 47 mm (w), 65.4 mm (L), 160 μm (D), and 218 μL (vol).

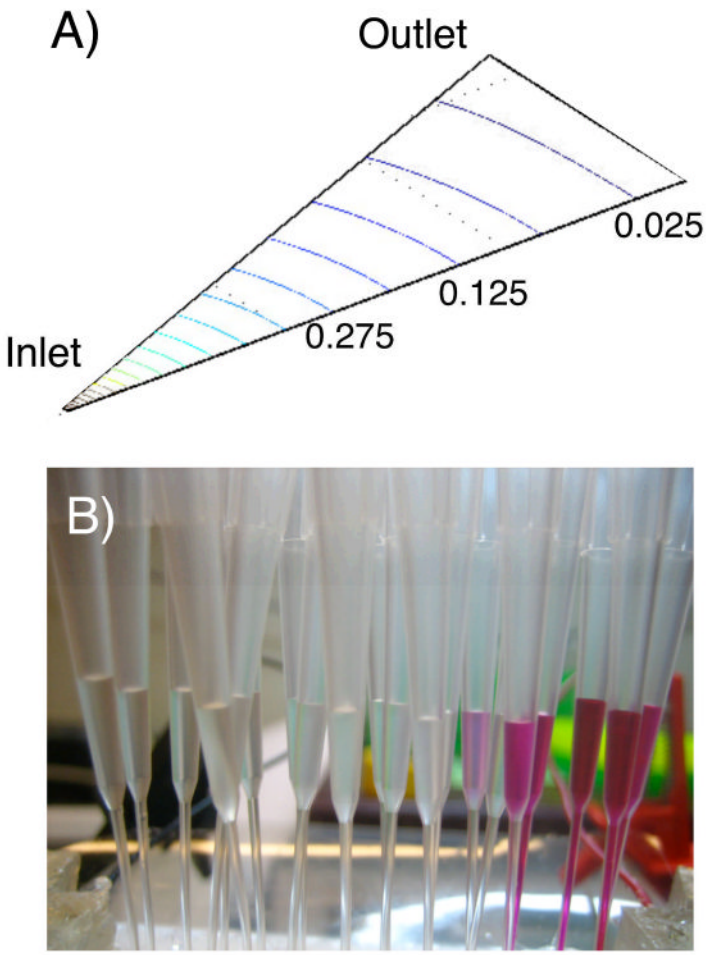

Figure 4.

A) FEMLAB two dimensional simulation of pressure drop in one half of the divergent device design. Only half of the channel was simulated due to the symmetry of the device. Isosurface pressure was valued between 0 and 1 with a step size of 0.05. B) Image of 24 outlet fractions after 0.5 mL of sample volume has been loaded (~20 μL of each fraction). Red color fractions represent the acidic region. Buffer: 50 mM Tris, 2% ampholytes 3-10, 0.1% Methyl Red, pH 7.5. Flow rate: 10 μL/min.

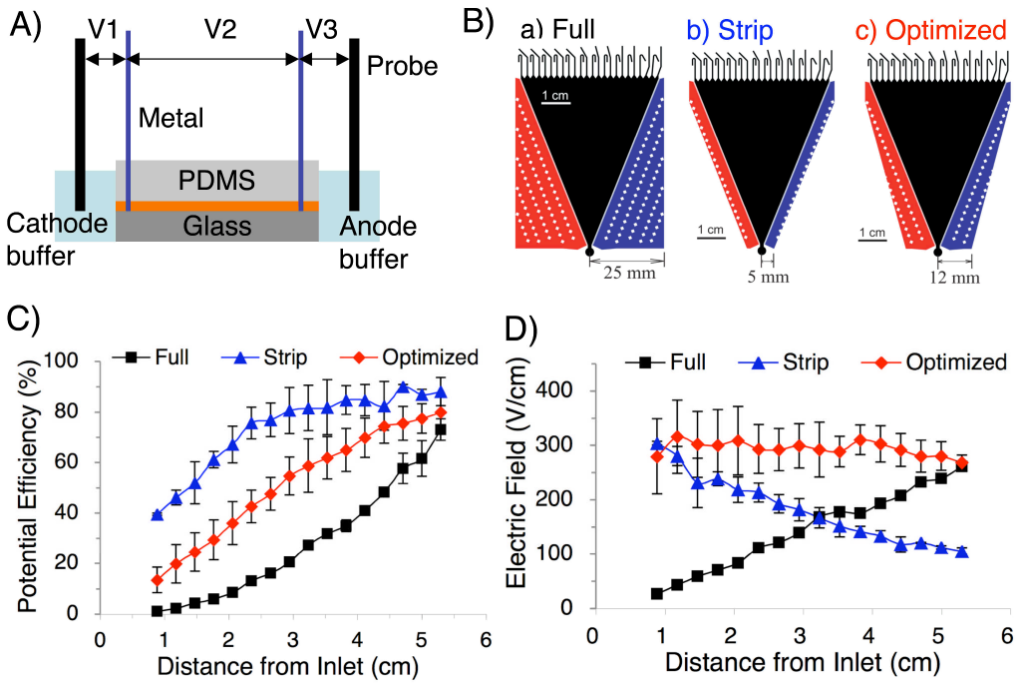

Figure 5.

Effect of poly (acrylamide) gel on the optimization of the electric field in aqueous buffer condition. A) Schematic drawing of potential measurement. B) Schemes of device designs. C) Cross-channel potential efficiency. D) Electric field measurements. Buffer: 50 mM Tris, 2% ampholytes 3-10, 0.1% Methyl Red, 0.1% Bromothymol Blue, pH 7.5. Flow rate: 10 μL/min. n = 3.

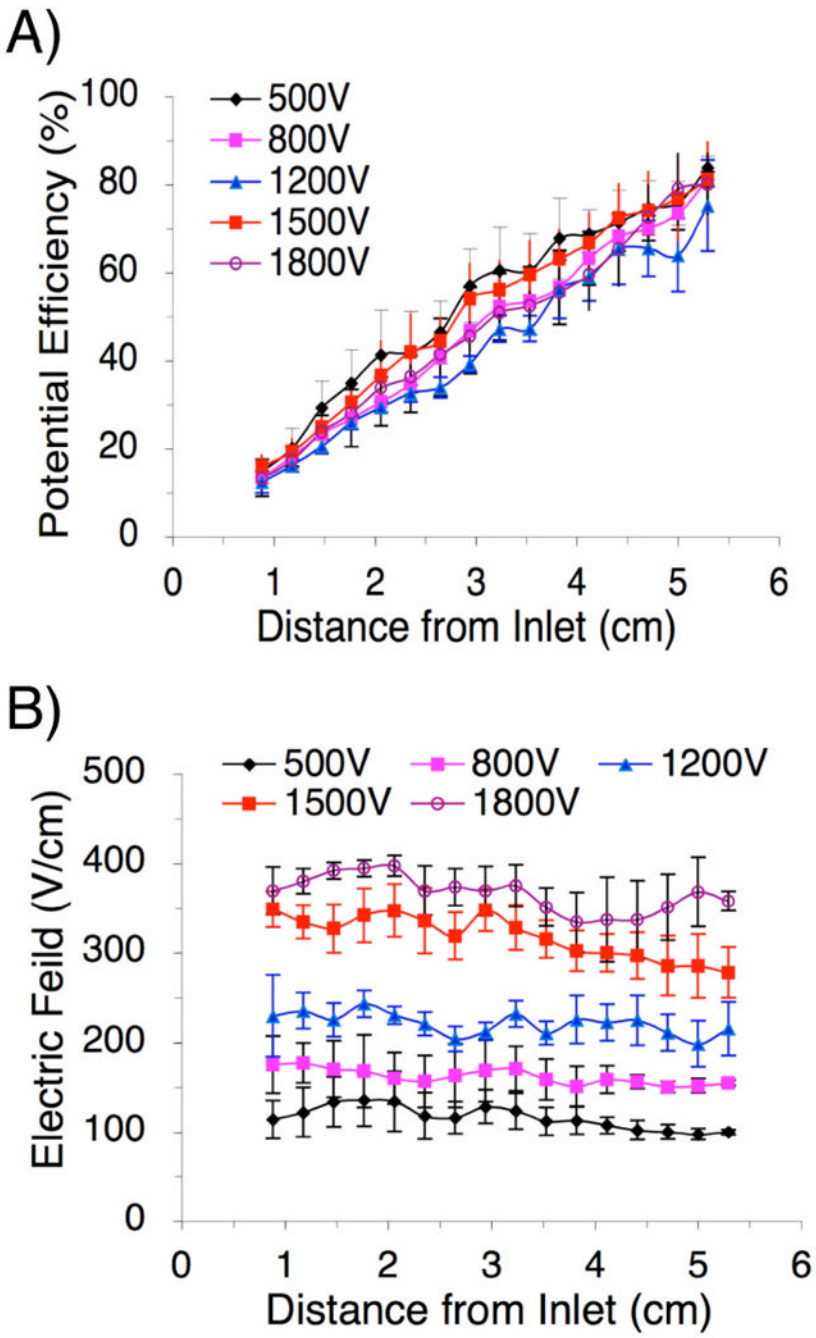

Figure 6.

A) Potential efficiency and B) Electric fields of FF-IEF system under urea denaturing buffer conditions. Sample buffer: 8 M Urea, 2 M thiourea, 4% CHAPS, 2% PVA, 0.1% Methyl Red. Flow rate: 10 μL/min. n = 5.

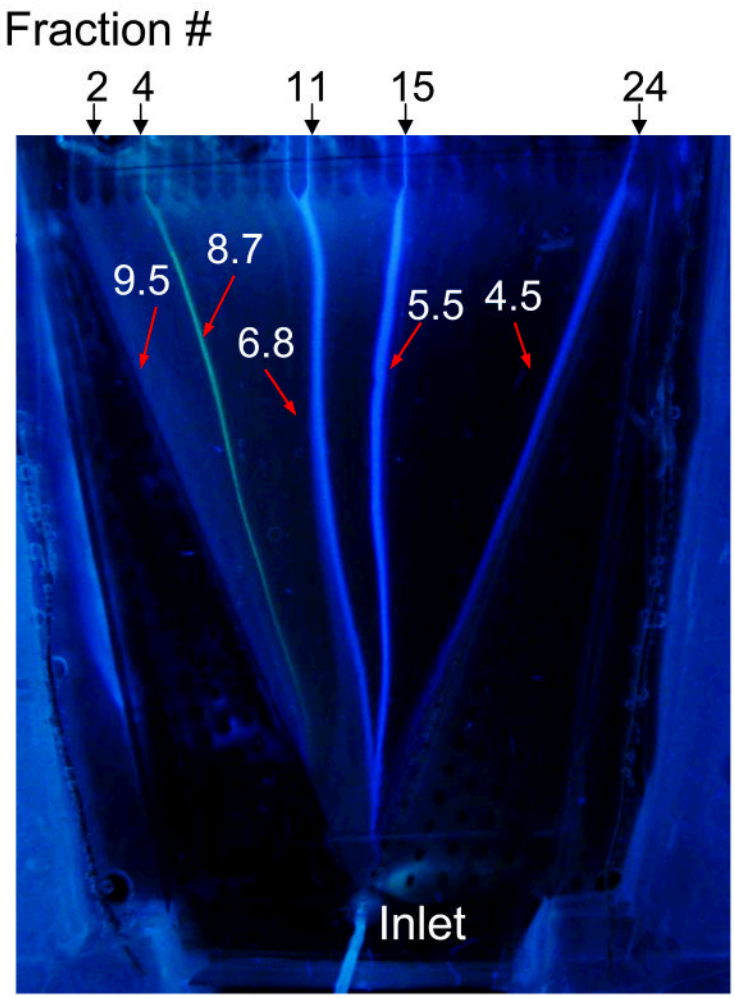

Figure 7.
Device images for separation of fluorescent pI markers, 9.5, 8.7, 6.8, 5.5, and 4.5. Buffer: 6 M Urea, 1.5 M Thiourea, 3% CHAPS, 4% PVA, 2% ampholytes. Applied voltage: 1800 V. Current: 1.3 mA. Flow rate: 10 μL/min. The device measures 50 mm by 75 mm, with the central triangular separation channel of 46 mm wide at the top and 56 mm long.